KS-Autoformer: An Autoformer-Based SOC Prediction Framework for Electric Vehicles

Yaoyidi Wang[1], Niansheng Chen[1], Lei Rao[1(✉)], Dingyu Yang[2], Guangyu Fan[1], Songlin Cheng[1], and Xiaoyong Song[1]

[1] Shanghai Dianji University, Shanghai 201306, China
raol@sdju.edu.cn
[2] Alibaba Group, Hangzhou 310056, China

Abstract. Accurate state of charge prediction is essential for battery management systems, which is crucial for improving battery utilization efficiency and ensuring safety performance. Current SOC prediction models only consider battery-related features but ignores vehicle information. Additionally, there are challenges preventing gradient disappearance and explosion during model training due to excessive data and noise. This paper introduces a new framework that integrates laboratory battery data with vehicle features to improve the accuracy of SOC. First, we apply Matlab/Simulink to simulate an electric vehicle and process the generated vehicle data with spearman correlation analysis to identify the most relevant features, such as the electric motor, differential, and aerodynamic drag. Then we develop a data fusion model to synchronize the heterogeneous datasets with different frequencies to capture the sudden change in electric vehicles. Furthermore, we propose a KS-Autoformer prediction model to address the overfitting problem caused by data redundancy and noise, which improves accuracy by smoothing sensor noise and enhancing time delay aggregation in an auto-correlation mechanism. Finally, we utilize different driving cycles for training and testing in order to effectively evaluate the extrapolation and adaptability of our model. Experimental results show that our model achieves a significant improvement in predicting SOC in terms of accuracy and robustness.

Keywords: State of Charge · Battery Management System · Autoformer

1 Introduction

Global emissions and pollution from transportation are increasing, and electric vehicles (EVs) are seen as the best solution to replace conventional internal combustion engine vehicles [1,2]. EVs use lithium-ion batteries (LIBs) for their

© ICST Institute for Computer Sciences, Social Informatics and Telecommunications Engineering 2024
Published by Springer Nature Switzerland AG 2024. All Rights Reserved
A. Zaslavsky et al. (Eds.): MobiQuitous 2023, LNICST 593, pp. 297–312, 2024.
https://doi.org/10.1007/978-3-031-63989-0_15

high voltage and power density, and are equipped with a battery management system (BMS) to regulate battery usage and scheduling, as well as monitor battery status and perform maintenance [3,4].

The State of charge (SOC) is defined as the ratio of the remaining capacity to the current maximum available capacity. Accurate prediction of the state of charge is an important step in BMS [5]. By accurate prediction of the state of charge, the BMS can help to prevent overcharging or undercharging of the battery [6], which would lead to decreased performance and a shorter lifespan. Since the internal battery chemistry is a complex process, the SOC prediction is susceptible to the battery discharge rate, ambient temperature, and battery degradation. Meanwhile, there exists a significant non-linear correlation between the external variables of an electric vehicle and its battery, which can make accurate SOC prediction challenging. For example, the aerodynamic drag coefficient of the electric vehicle varies with its speed, and the mechanical power loss of the motor can result in faster battery discharge, further contributing to inaccurate SOC prediction.

Researchers have proposed various methods for SOC prediction, including traditional methods, model-based methods, and data-driven methods.

Traditional methods include the Ampere-hour integration method [7,8] and the open-circuit voltage method [9,10]. These methods are still used in commercial electric vehicles because of their simplicity and low computational resource requirements. The Ampere-hour integration method predicts SOC by integrating the discharge current over time, but it has a strong dependence on the accuracy of the initial SOC value. Moreover, measurement errors can accumulate over time due to low-precision current sensors, resulting in increasingly inaccurate SOC prediction. The open-circuit voltage (OCV) method predicts SOC by measuring the battery's OCV and checking the OCV-SOC curve, but the battery's OCV can only be obtained by long-term offline maintenance, making this method difficult to predict SOC in real-time. Therefore, traditional methods have limitations on low precision and difficulty in real-time application.

A model-based method using an equivalent circuit model (ECM) [11] has been proposed to predict the state of a battery. This method applies the ampere-hour integration approach based on the last moment SOC to predict the current SOC. The simulated voltage of the battery, combined with the equivalent circuit model, is then used to predict the SOC. An adaptive filter is introduced to calibrate the prediction of SOC by continuously reducing the error between the simulated value and the actual measured voltage, which creates a closed-loop SOC prediction. Common ECM models include the PNGV model [12], Thevenin model [13], and second-order RC model [14,15]. Common adaptive filtering algorithms include particle filtering [16,17], extended Kalman filtering (EKF) [18,19], unscented Kalman filtering (UKF) [20,21], and cubature Kalman filtering (CKF) [22,23]. While this method can fix initial errors and avoid error accumulation over time, it has poor adaptability to resistance and capacitance parameters. Additionally, it ignores the internal chemical characteristics of the battery and nonlinear errors in the equivalent model.

The data-driven method is a machine learning approach that uses historical battery usage data to predict the state of charge (SOC) of the battery [24, 25]. This method does not require any knowledge of the internal workings of the battery and can be easily implemented by inputting training data into a data-driven model. Statistical learning methods such as support vector machines (SVM) [26] and Gaussian process regression (GPR) [27,28] are faster and more computationally efficient, making them more suitable for sparse features.

However, existing SOC prediction frameworks have several limitations that need to be addressed, including:

(I) Current battery input data cannot reflect the sudden changes in operating conditions of electric vehicles. Tian et al. [29] proposed a DNN approach for SOC prediction in EVs using data from a 10-minute charging session, which consists of convolutional layers, GRU layers and dense layer. Huang et al. [30] developed a hybrid neural networks CNN-GRU model using single time-point measurements of voltage, current, and temperature. However, battery SOC fluctuate significantly during acceleration and deceleration of vehicle, making it difficult for models trained on single-time-point or longer-duration data to capture sufficient temporal information.

(II) External vehicle conditions are not considered in predicting SOC. Previous studies on SOC prediction mainly used laboratory battery data as input variables. Furthermore, in actual EV operations, it is hard to obtain external conditions that affect battery discharge due to cost and feasibility constraints. Huang et al. [31] used real-world vehicle data from NDANEV but equalized battery degradation effects with vehicle driving mileage. Li et al. [32] integrated weather and vehicle data and used a novel dual-dropout-based neural network to predict SOC. Although these studies considered the impact of vehicle data on SOC prediction, they were both suffered from significant data loss and sampling limitations.

(III) Current SOC prediction models fail to address overfitting from large data and noise. The noise in battery data collection and the overfitting caused by large data will result in unstable SOC prediction and reduced accuracy, which affects EV safety and driving range.

Therefore, the main contributions of this paper are as follows:

(I) A novel SOC prediction framework: a simulation model of an electric vehicle is built using Matlab/Simulink, which incorporates external vehicle data and laboratory battery data to establish the relationship between external vehicle conditions and battery consumption. To the best of our knowledge, we are the first to formulate this framework that can be customized for specific vehicle operating conditions by inputting corresponding driving cycles and electric vehicle parameters.

(II) A data fusion method for heterogeneous datasets with different frequencies: We resample the data to capture the sudden change of electric vehicles with features in our simulation and enhance the robustness of the trained model for complex battery conditions.

(III) We propose a KS-Autoformer model, which utilizes decomposition architectures to handle large amounts of data. The Auto-Correlation attention mechanism is used to better predict the SOC of electric vehicles under driving cycles. Moreover, we apply Kalman smoothing using a recursive algorithm to filter and eliminate noise from laboratory-collected battery discharge data.

(IV) We applied our framework to different driving cycles for training and testing. Through comparison and ablation experiments, we show that our proposed framework and prediction model can achieve more accurate SOC predictions.

2 Prediction Framework for Electric Vehicle

In this section, we describe the details of our prediction framework of SOC. It includes three modules: laboratory battery data and simulated external vehicle data generation, data fusion utilizing high-frequency sampling data, and a deep-learning based prediction model called *KS-Autoformer*. The proposed framework is illustrated in Fig. 1. We first outline the process of constructing an electric vehicle simulation and analyze the generated features to identify the most related information. Next, we will introduce the fusion of laboratory battery and simulated external vehicle data, which finally will be performed in our proposed prediction model *KS-Autoformer*.

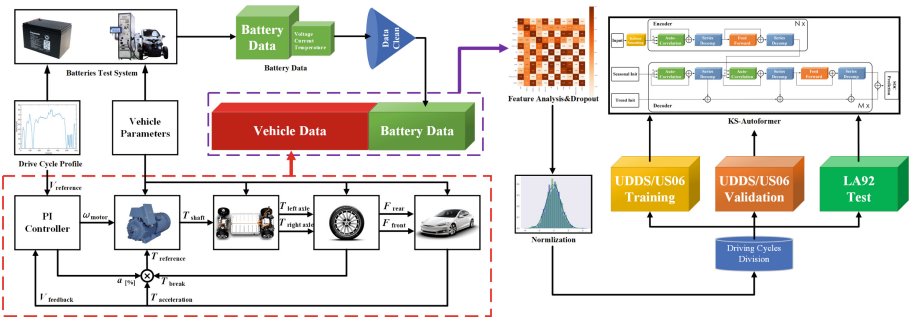

Fig. 1. The overview of SOC prediction architecture

2.1 Electric Vehicle Simulation

Since it is difficult to measure or obtain vehicle data (such as losses in the electric motor, power system, and air resistance) in real systems, we conduct a simulation of an electric vehicle model using Matlab/Simulink [33]. Simulink's Powertrain Blockset [34,35] is a powerful computational tool that has been widely used in simulations and analysis of vehicle dynamics. The Powertrain Blockset consists of several blocks that are designed to calculate various aspects of the motor system.

In order to generate the electric motor's mechanical power data W_{motor}, we utilize the Mapped Motor block to control the output shaft torque T_{shaft}, based on the reference torque $T_{\text{reference}}$. This reference torque is determined by the acceleration torque $T_{\text{acceleration}}$ and braking torque T_{brake}.

Next, the Limited Slip Differential and Longitudinal Wheel blocks are used to calculate the corresponding torques $T_{\text{left axle}}$ and $T_{\text{right axle}}$ and the net longitudinal forces F_{rear} and F_{front} acting on the rear and front wheels, respectively, which allow us to determine the mechanical power transferred through the differential W_{differ}.

By utilizing the Vehicle Body 1DOF Longitudinal block, which considers the feedback speed V_{feedback} and acceleration torque $T_{\text{acceleration}}$, we are able to obtain the mechanical power transferred from the axle to the wheel W_{wheel}, as well as the power loss due to rolling resistance W_{roll}, the mechanical power required for braking W_{break}, and the power loss due to wind resistance W_{wind}.

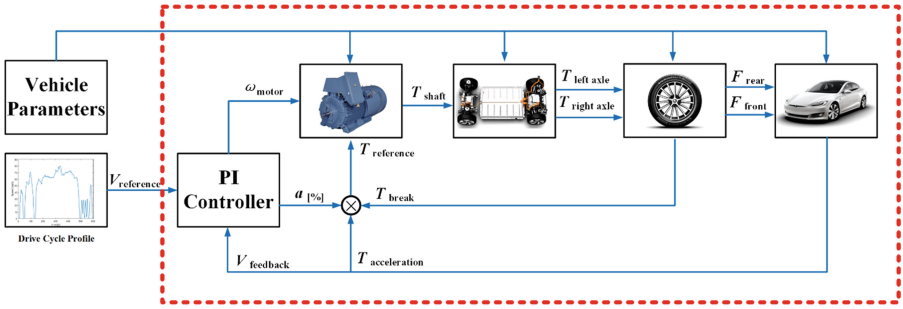

Fig. 2. Schematic of the EV model using Matlab/Simulink.

To summarize, these blocks are used to simulate the powertrain system and vehicle dynamics of an electric vehicle. A schematic of the EV model is designed and presented in Fig. 2. The mechanical power of the motor W_{motor}, power transferred through the differential W_{differ}, power transferred from axle to wheel W_{wheel}, power loss due to rolling resistance W_{roll}, power required for braking W_{break}, and power loss due to wind resistance W_{wind} will be output as a part of the vehicle data. These components are widely recognized and utilized as essential features within real-world automotive datasets.

2.2 Feature Analysis

In the previous section, we obtain various features of the electric vehicle model including W_{motor}, W_{differ}, W_{wheel}, W_{roll}, W_{break}, and W_{wind}. However, it is important to note that not all vehicle features are equally relevant to the battery SOC, and the inclusion of irrelevant features in the dataset may result in overfitting. Therefore, a feature analysis is necessary to identify the most relevant characteristics for accurate SOC prediction.

To analyze the features, we utilize the Spearman correlation coefficient [36], which is ideal for SOC data that displays a monotonic decay. The coefficient measures the strength and direction of the monotonic relationship between two variables, as defined by the formula:

$$\rho = 1 - \frac{6\sum_{i=1}^{n} d_i^2}{n\left(n^2 - 1\right)} \tag{1}$$

where d is the difference in ranks between the two variables, and n is the number of data points. This method does not assume a linear relationship or a specific distribution form, making it more suitable for evaluating the correlation between features and battery SOC, especially when dealing with monotonic data.

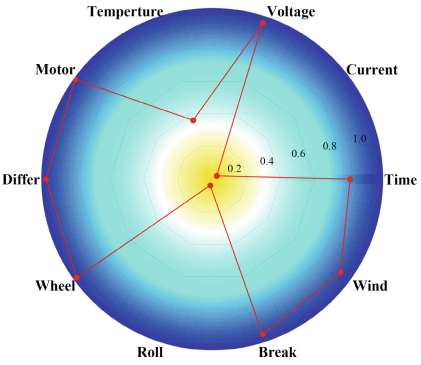

Fig. 3. Spearman correlation coefficient between different features and SOC.

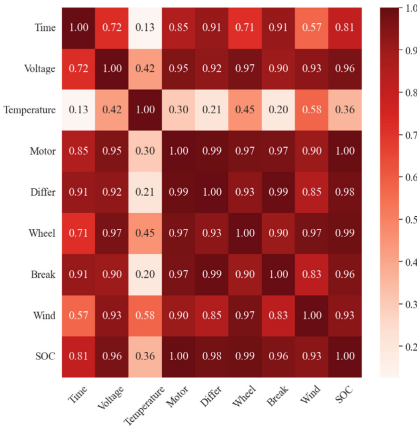

Fig. 4. Spearman correlation coefficient of selected features.

In Fig. 3, we observe that the Current in battery data and the power loss W_{roll} due to rolling resistance in vehicle data both have a low correlation coefficient of 0.02 and 0.03. Hence, we drop these two irrelevant features from our dataset. Then, we conduct a secondary correlation analysis on the remaining features, and as shown in Fig. 4, select eight relevant features for SOC prediction. This approach helps to eliminate irrelevant features and reduces the data size, thereby avoiding the overfitting of the model.

2.3 Data Fusion

To integrate the battery data and simulated external vehicle condition data, we employ a data fusion technique to match the spatial and temporal dimensions of the datasets.

For spatial matching, we use the vehicle parameters and driving cycle as the connection link. Specifically, we input the driving cycles and vehicle parameters used in the battery discharge tests (UDDS, US06 and LA92) into the simulation model to ensure the consistency of the data in the test environment.

For temporal matching, we first interpolate the missing battery data as it is collected in the laboratory using the sensor. We utilize the Lagrange interpolation method [37]. Assuming that the battery dataset consists of n-time data points. The Lagrange interpolation formula is:

$$l_i\left(x_{missing}\right) = \prod_{j=1, j\neq i}^{n} \frac{x_{missing} - x_j}{x_i - x_j} \tag{2}$$

where $l_i\left(x_{missing}\right)$ is the Lagrange interpolation basis function:

$$y_{missing} = \sum_{i=1}^{n} y_i \cdot l_i\left(x_{missing}\right) \tag{3}$$

By interpolating the missing data, we ensure that the battery data is a complete sample with a fixed sampling frequency of 10 Hz. We then set the simulation model's vehicle data sampling frequency to match the same rate of 10 Hz. This allows us to fuse the battery data and simulated vehicle data for SOC prediction.

2.4 Prediction Model

The KS-Autoformer module, as depicted in Fig. 5, is composed of three essential parts: the decomposition architecture, the auto-correlation mechanism, and the Kalman smoothing technique.

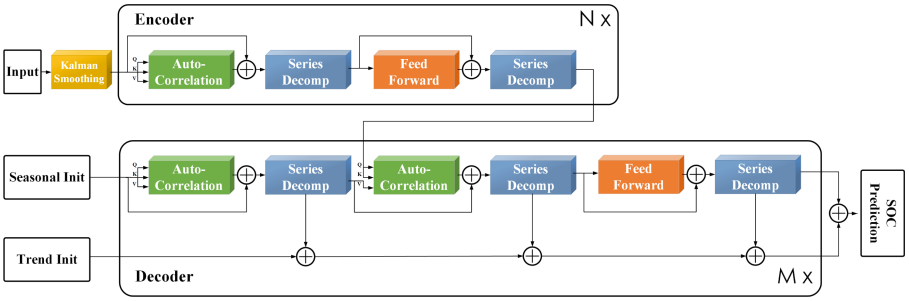

Fig. 5. Structure of KS-Autoformer.

Decomposition Block. Decomposition can help to separate the seasonal and trend components of our dataset. By doing so, we can better understand the stable and fluctuating patterns of the electric vehicle's behavior. Furthermore, it

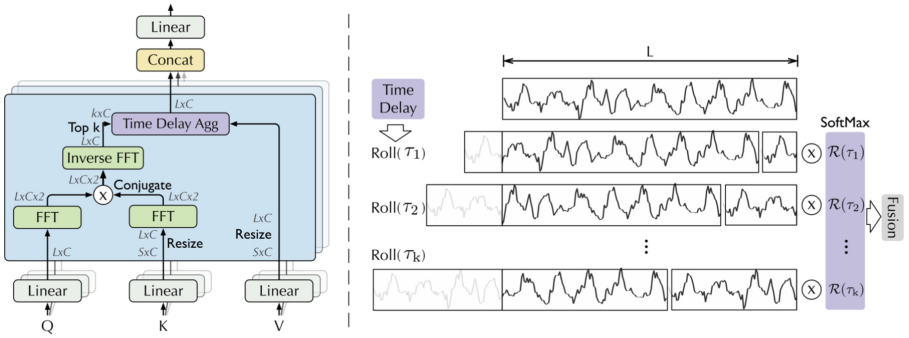

Fig. 6. Auto-Correlation (left) and Time delay aggregation (right).

simplifies the training process and reduces the risk of overfitting. For a Length L time series $X \in \mathbb{R}^{L \times d}$, the decomposition can be expressed as:

$$\begin{aligned} X_t &= AvgPool(Padding(X)) \\ X_s &= X - X_t \end{aligned} \tag{4}$$

where $X_s, X_t \in \mathbb{R}^{L \times d}$ represent the seasonal and trends part severally. AvgPool(X) combined with a padding method is exploited as the moving average operation. As a result, the whole process of decomposition can be expressed as:

$$X_s, X_t = SeriesDecomp(X) \tag{5}$$

Auto-correlation Mechanism. The Auto-Correlation mechanism [38] is taking the place of the canonical self-attention mechanism which is shown in Fig. 6. The historical sub-sequences of battery data often contain important information about the current battery state. To model the similarities between the subsequences, suppose a real-time discrete series $\{X_t\}$, the auto-correlation $R_{XX}(\tau)$ is proposed, which can be expressed as:

$$R_{XX}(\tau) = \lim_{L \to +\infty} \frac{1}{L} \sum_{t=1}^{L} X_t X_{t-\tau} \tag{6}$$

where $R_{XX}(\tau)$ measures the time lag similarities between $\{X_t\}$ and the lag τ series $\{X_{t-\tau}\}$. After the calculation process, the top k possible temporal series $\tau_1, \tau_2, \ldots, \tau_k$ are selected and can be expressed as:

$$\tau_1, \cdots, \tau_k = argTopk_{\tau \in 1, \cdots, L_{seq}} \left(R_{Q,K}(\tau) \right) \tag{7}$$

To achieve sequence-level joins, similar subsequence information needs to be aggregated. As shown in Fig. 6, according to the predicted cycle length, the Roll(·) operation is first used for information alignment, and then the information aggregation is carried out, and the form of query, key, and value are still used here.

$$\hat{R}_{Q,K}(\tau_1), \cdots, \hat{R}_{Q,K}(\tau_k) = SoftMax\left(\hat{R}_{Q,K}(\tau_1), \cdots, \hat{R}_{Q,K}(\tau_k)\right) \quad (8)$$

$$Auto - Correlation(Q, K, V) = \sum_{i=1}^{k} Roll(V, \tau_k)\, \hat{R}_{Q,K}(\tau_k) \quad (9)$$

Kalman Smoothing. To enhance the time delay aggregation technique described earlier, we employed Kalman smoothing, a mathematical method used to reduce noise and preserve the original patterns in laboratory battery data. The application of Kalman smoothing involves utilizing the following equation:

$$x_{k|k-1}\& = F_k x_{k-1|k-1} + B_k u_k \quad (10)$$

$$P_{k|k-1}\& = F_k P_{k-1|k-1} F_k^T + Q_k \quad (11)$$

$$K_k\& = P_{k|k-1} H_k^T (H_k P_{k|k-1} H_k^T + R_k)^{-1} \quad (12)$$

$$x_{k|k}\& = x_{k|k-1} + K_k(y_k - H_k x_{k|k-1}) \quad (13)$$

$$P_{k|k}\& = (I - K_k H_k) P_{k|k-1} \quad (14)$$

where $x_{k|k}$ is the a predict of the state, F_k is the state transition matrix, B_k is the input matrix, u_k is the input vector, $P_{k|k-1}$ is the a priori predict error covariance matrix, Q_k is the process noise covariance matrix, K_k is the Kalman gain, y_k is the measurement vector. H_k is the observation matrix, R_k is the measurement noise covariance matrix.

In Fig. 7, Kalman smoothing is shown to have improved the quality of laboratory battery data by reducing noise while preserving temporal patterns. This enhanced data can be used to improve time delay aggregation, a technique introduced above to summarize temporal data. Kalman smoothing produces a more accurate representation of the process, which leads to more precise aggregated values. It also helps to reduce the impact of outliers and anomalies in the data, improving the robustness of time delay aggregation results.

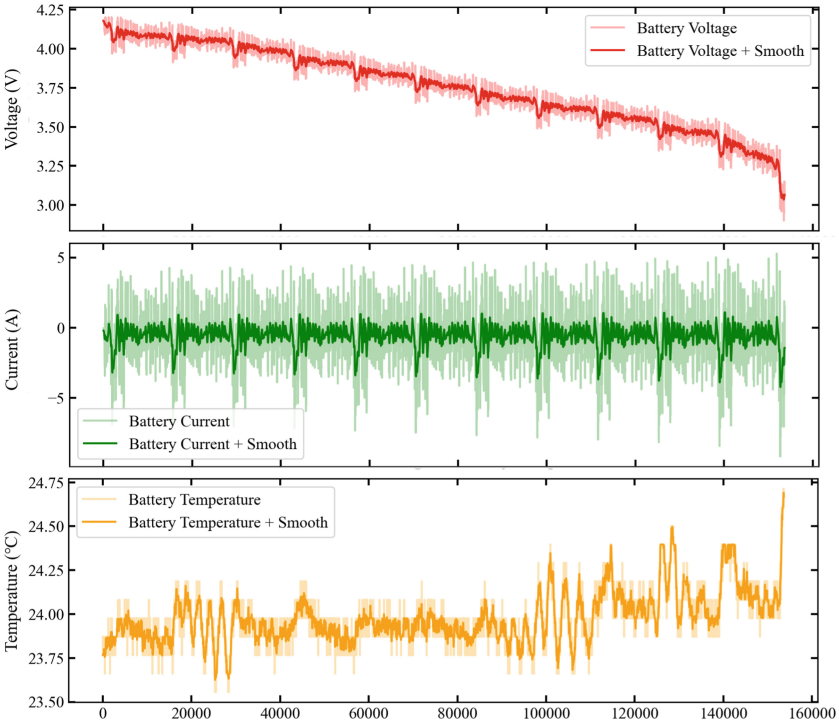

Fig. 7. Kalman smoothing on [a] Voltage; [b] Current; [c] Temperature.

3 Experimental Evaluation

Dataset. We employed the LG Open Battery Dataset [39] and applied it within the framework proposed in our research. Figure 8 displays the operational data of a 3Ah LG 18650 battery under the UDDS driving cycle, accompanied by the vehicle's external data obtained using our framework. In order to more effectively evaluate the extrapolation and adaptability of the model, we select specific driving cycles to form the training and validation sets and use the data from another DC for testing. In this research paper, we employ the UDDS and US06 driving cycles to form the training and validation sets. The UDDS and US06 driving cycles are chosen due to their ability to represent typical urban driving conditions, encompassing factors such as stop-and-go traffic and moderate acceleration patterns. Additionally, the US06 driving cycle specifically captures aggressive and high-speed/acceleration driving behavior, incorporating rapid speed fluctuations. To assess the model's performance on unseen data, we employ the LA92 driving cycle as the test dataset.

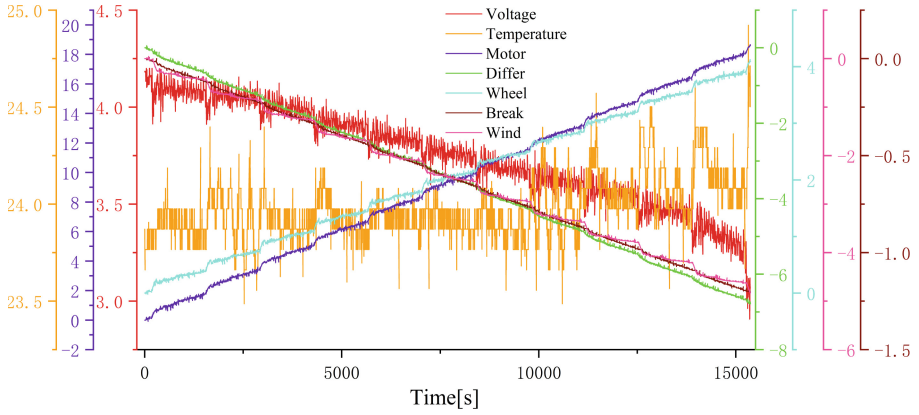

Fig. 8. Illustration of battery and vehicle dataset.

Evaluation Metrics. SOC prediction can be evaluated using various metrics, including MSE, RMSE, and MAE. These metrics provide quantitative measures of how well an prediction algorithm is performing compared to actual SOC values.

MSE (Mean Squared Error) formula is:

$$\mathrm{MSE} = \frac{1}{N}\sum_{i=1}^{N}(SOC_{\mathrm{est}} - SOC_{\mathrm{act}})^2 \tag{15}$$

where SOC_{est} is the predicted value, SOC_{act} is the true value, and N is the number of samples. MSE provides a simple and straightforward expression for prediction error, but squaring the error value amplifies the impact of outliers.

RMSE (Root Mean Squared Error) formula is:

$$\mathrm{RMSE} = \sqrt{\frac{1}{N}\sum_{i=1}^{N}(SOCest - SOCact)^2} \tag{16}$$

RMSE is essentially the square root of MSE, which helps to ensure that the evaluation metric is consistent with the original value scale.

MAE (Mean Absolute Error) formula is:

$$\mathrm{MAE} = \frac{1}{N}\sum_{i=1}^{N}|SOCest - SOCact| \tag{17}$$

MAE maintains consistency between the scale of the error metric and the original values, and does not suffer from the issue of error amplification due to squaring.

Implementation. To ensure fair and meaningful comparisons between the KS-Autoformer model and other models, we employed consistent hyperparameter

settings as foo: an initial learning rate of 0.0001, p = 0.05 dropout, and a batch size of 32. The size of each input time series segment is 96, and the prediction horizon is set to 24. The training process is terminated after six epochs, and we repeat each experiment five times to ensure the reliability of the results. Also, we compute the mean and standard deviation of the different datasets to normalize all the data points. In the end, we conduct experiments on a workstation equipped with a GeForce RTX 3070 GPU and an AMD Ryzen 7 5800 CPU.

Comparative Experiment. In our experiments, we conduct a comparative analysis between KS-Autoformer and several baseline models, including Autoformer, Informer, and Transformer. The results are displayed in Fig. 9. This experiment reveals that KS-Autoformer outperforms the baseline Autoformer model in predicting the state of charge of electric vehicle batteries since our model addresses sensor data noise and improves time delay aggregation in the Auto-correlation mechanism. Moreover, our proposed model performs better than other Transformer models, such as Informer and the original Transformer model.

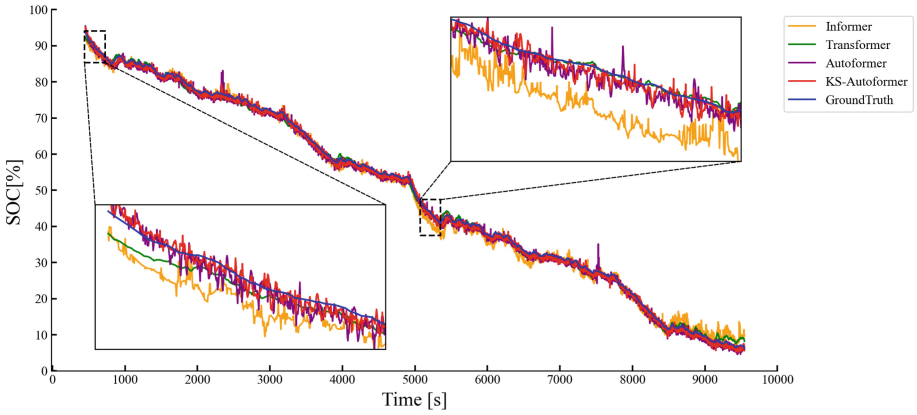

Fig. 9. Performance of different SOC prediction models.

Ablation Experiment. To demonstrate the validity of the proposed SOC prediction framework, we conducted another ablation experiment. Specifically, we compared our proposed model with three other baseline models under both the original SOC prediction framework and the proposed SOC prediction framework, as shown in Table 1 and Fig. 10. The results indicate that all four algorithms outperformed the original SOC prediction framework.

Table 1. Comparison of models in different frameworks.

Model	Framework	MSE [%]	RMSE [%]	MAE [%]
KS-Autoformer	Origin	0.0228	1.5099	0.7974
	Proposed	**0.0083**	**0.9149**	**0.7295**
Autoformer [38]	Origin	0.0257	1.6061	0.6290
	Proposed	**0.0157**	**1.2540**	**0.7876**
Informer [40]	Origin	0.0698	2.6426	2.1114
	Proposed	**0.0681**	**2.6096**	**1.9711**
Transformer [41]	Origin	0.0475	2.1802	1.1241
	Proposed	**0.0439**	**1.9227**	**1.0886**

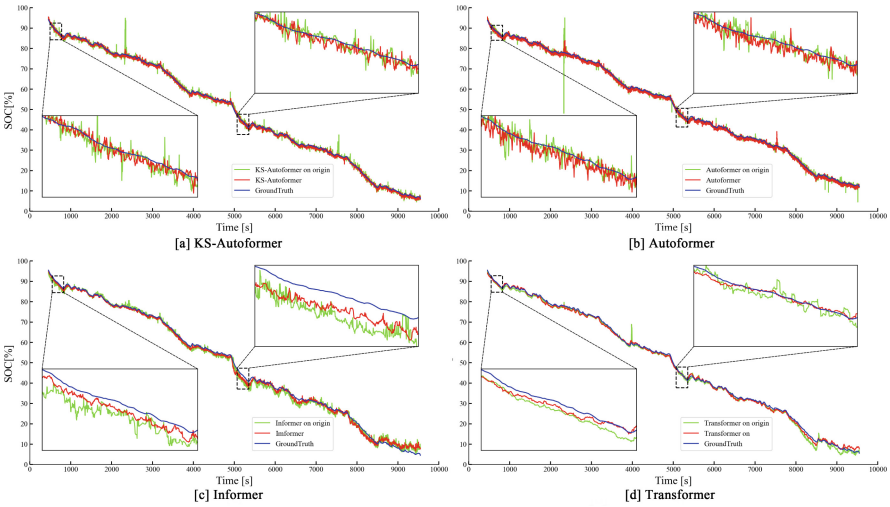

Fig. 10. Performance of different framework on [a] KS-Autoformer; [b] Autoformer; [c] Informer; [d] Transformer.

4 Conclusion

In this work, we propose a novel framework for predicting the state of charge of electric vehicle batteries, incorporating external vehicle data and laboratory battery data. After features analysis and data fusion, our high-frequency sampling dataset can capture sufficient temporal information under complex operating conditions. Furthermore, we propose a KS-Autoformer prediction model to address issues related to feature explosion and reduce sensor measurement errors. In order to more effectively evaluate the extrapolation and adaptability of our model, UDDS and US06 driving cycles are used for training and LA92 driving cycle for testing. Results show that our proposed framework achieves superior performance in predicting SOC, leading to more efficient battery utilization and improved safety performance.

References

1. Yang, F., Wang, D., Zhao, Y., Tsui, K.L., Bae, S.J.: A study of the relationship between coulombic efficiency and capacity degradation of commercial lithium-ion batteries. Energy **145**, 486–495 (2018). https://doi.org/10.1016/j.energy.2017.12.144. https://www.sciencedirect.com/science/article/pii/S0360544217321874
2. Xu, Y., et al.: Research on the impact of re-electrication in the transportation sector on carbon emission and pollutant emission in Yunnan province. In: 2021 Power System and Green Energy Conference (PSGEC), pp. 407–412. IEEE (2021)
3. Hannan, M.A., Lipu, M.H., Hussain, A., Mohamed, A.: A review of lithium-ion battery state of charge estimation and management system in electric vehicle applications: challenges and recommendations. Renew. Sustain. Energy Rev. **78**, 834–854 (2017)
4. Rahimi-Eichi, H., Ojha, U., Baronti, F., Chow, M.Y.: Battery management system: An overview of its application in the smart grid and electric vehicles. IEEE Ind. Electron. Mag. **7**(2), 4–16 (2013)
5. Zhang, D., Zhong, C., Xu, P., Tian, Y.: Deep learning in the state of charge estimation for li-ion batteries of electric vehicles: a review. Machines **10**(10), 912 (2022). https://doi.org/10.3390/machines10100912. https://www.mdpi.com/2075-1702/10/10/912
6. Zhou, W., Zheng, Y., Pan, Z., Lu, Q.: Review on the battery model and SOC estimation method. Processes **9**(9), 1685 (2021)
7. Zhang, X., Hou, J., Wang, Z., Jiang, Y.: Study of SOC estimation by the ampere-hour integral method with capacity correction based on LSTM. Batteries **8**(10), 170 (2022)
8. Deng, Y., Hu, Y., Cao, Y.: An improved algorithm of SOC testing based on open-circuit voltage-ampere hour method. In: Li, K., Xue, Y., Cui, S., Niu, Q. (eds.) LSMS/ICSEE 2014. CCIS, vol. 463, pp. 258–267. Springer, Heidelberg (2014). https://doi.org/10.1007/978-3-662-45286-8_27
9. Tian, J., Xiong, R., Shen, W., Sun, F.: Electrode ageing estimation and open circuit voltage reconstruction for lithium ion batteries. Energy Storage Mater. **37**, 283–295 (2021)
10. Pillai, P., Sundaresan, S., Kumar, P., Pattipati, K.R., Balasingam, B.: Open-circuit voltage models for battery management systems: a review. Energies **15**(18), 6803 (2022)
11. Xile, D., Caiping, Z., Jiuchun, J.: Evaluation of SOC estimation method based on EKF/AEKF under noise interference. Energy Procedia **152**, 520–525 (2018)
12. Liu, X., Li, W., Zhou, A.: PNGV equivalent circuit model and SOC estimation algorithm for lithium battery pack adopted in AGV vehicle. IEEE Access **6**, 23639–23647 (2018)
13. Susanna, S., Dewangga, B.R., Wahyungoro, O., Cahyadi, A.I.: Comparison of simple battery model and thevenin battery model for SOC estimation based on OCV method. In: 2019 International Conference on Information and Communications Technology (ICOIACT), pp. 738–743. IEEE (2019)
14. Ji, Y., Qiu, S., Li, G.: Simulation of second-order RC equivalent circuit model of lithium battery based on variable resistance and capacitance. J. Cent. South Univ. **27**(9), 2606–2613 (2020)
15. Xu, Y., Hu, M., Fu, C., Cao, K., Su, Z., Yang, Z.: State of charge estimation for lithium-ion batteries based on temperature-dependent second-order RC model. Electronics **8**(9), 1012 (2019)

16. Burgos-Mellado, C., Orchard, M.E., Kazerani, M., Cárdenas, R., Sáez, D.: Particle-filtering-based estimation of maximum available power state in lithium-ion batteries. Appl. Energy **161**, 349–363 (2016)
17. Xiong, R., Zhang, Y., He, H., Zhou, X., Pecht, M.G.: A double-scale, particle-filtering, energy state prediction algorithm for lithium-ion batteries. IEEE Trans. Ind. Electron. **65**(2), 1526–1538 (2017)
18. Plett, G.L.: Dual and joint EKF for simultaneous SOC and SOH estimation. In: Proceedings of the 21st Electric Vehicle Symposium (EVS21), Monaco, pp. 1–12 (2005)
19. Li, M., Zhang, Y., Hu, Z., Zhang, Y., Zhang, J.: A battery SOC estimation method based on AFFRLS-EKF. Sensors **21**(17), 5698 (2021)
20. El Din, M.S., Hussein, A.A., Abdel-Hafez, M.F.: Improved battery SOC estimation accuracy using a modified UKF with an adaptive cell model under real EV operating conditions. IEEE Trans. Transp. Electrification **4**(2), 408–417 (2018)
21. He, H., Qin, H., Sun, X., Shui, Y.: Comparison study on the battery SoC estimation with EKF and UKF algorithms. Energies **6**(10), 5088–5100 (2013)
22. Tao, Z., Li, Z., Yangcheng, H.O.U., Wei, C.: SOC estimation of aging lithium battery based on adaptive CKF. Energy Storage Sci. Technol. **9**(4), 1193 (2020)
23. Luo, J., Peng, J., He, H.: Lithium-ion battery SOC estimation study based on Cubature Kalman filter. Energy Procedia **158**, 3421–3426 (2019)
24. Cai, L., Meng, J., Stroe, D.I., Peng, J., Luo, G., Teodorescu, R.: Multiobjective optimization of data-driven model for lithium-ion battery SOH estimation with short-term feature. IEEE Trans. Power Electron. **35**(11), 11855–11864 (2020)
25. How, D.N., Hannan, M.A., Lipu, M.H., Ker, P.J.: State of charge estimation for lithium-ion batteries using model-based and data-driven methods: a review. IEEE Access **7**, 136116–136136 (2019)
26. Antón, J., Nieto, P.G., de Cos Juez, F.J., Lasheras, F.S., Vega, M.G., Gutiérrez, M.R.: Battery state-of-charge estimator using the SVM technique. Appl. Math. Model. **37**(9), 6244–6253 (2013)
27. Ozcan, G., Pajovic, M., Sahinoglu, Z., Wang, Y., Orlik, P.V., Wada, T.: Online state of charge estimation for lithium-ion batteries using gaussian process regression. In: IECON 2016-42nd Annual Conference of the IEEE Industrial Electronics Society, pp. 998–1003. IEEE (2016)
28. Sahinoglu, G.O., Pajovic, M., Sahinoglu, Z., Wang, Y., Orlik, P.V., Wada, T.: Battery state-of-charge estimation based on regular/recurrent Gaussian process regression. IEEE Trans. Ind. Electron. **65**(5), 4311–4321 (2017)
29. Tian, J., Xiong, R., Shen, W., Lu, J.: State-of-charge estimation of LiFePO4 batteries in electric vehicles: a deep-learning enabled approach. Appl. Energy **291**, 116812 (2021)
30. Huang, Z., Yang, F., Xu, F., Song, X., Tsui, K.L.: Convolutional gated recurrent unit-recurrent neural network for state-of-charge estimation of lithium-ion batteries. IEEE Access **7**, 93139–93149 (2019)
31. Huang, S., He, Z., Li, X.: A method of SOC estimation for electric vehicle based on limited information. In: 2020 IEEE International Conference on Networking, Sensing and Control (ICNSC), pp. 1–4. IEEE (2020). https://doi.org/10.1109/ICNSC48988.2020.9238124. https://ieeexplore.ieee.org/document/9238124/
32. Li, R., Wang, H., Dai, H., Hong, J., Tong, G., Chen, X.: Accurate state of charge prediction for real-world battery systems using a novel dual-dropout-based neural network. Energy **250**, 123853 (2022). https://doi.org/10.1016/j.energy.2022.123853. https://linkinghub.elsevier.com/retrieve/pii/S0360544222007563

33. Kasera, J., Chaplot, A., Maherchandani, J.K.: Modeling and simulation of wind-PV hybrid power system using Matlab/Simulink. In: 2012 IEEE Students' Conference on Electrical, Electronics and Computer Science, pp. 1–4. IEEE (2012)
34. Tran, M.K., Akinsanya, M., Panchal, S., Fraser, R., Fowler, M.: Design of a hybrid electric vehicle powertrain for performance optimization considering various powertrain components and configurations. Vehicles **3**(1), 20–32 (2020)
35. Ragone, M., Yurkiv, V., Ramasubramanian, A., Kashir, B., Mashayek, F.: Data driven estimation of electric vehicle battery state-of-charge informed by automotive simulations and multi-physics modeling. J. Power Sources **483**, 229108 (2021)
36. Myers, L., Sirois, M.J.: Spearman correlation coefficients, differences between **12** (2014)
37. Rashed, M.T.: Lagrange interpolation to compute the numerical solutions of differential, integral and integro-differential equations. Appl. Math. Comput. **151**(3), 869–878 (2004)
38. Wu, H., Xu, J., Wang, J., Long, M.: Autoformer: decomposition transformers with auto-correlation for long-term series forecasting (2021). http://arxiv.org/abs/2106.13008
39. Kollmeyer, P., Vidal, C., Naguib, M., Skells, M.: LG 18650hg2 li-ion battery data and example deep neural network xEV SOC estimator script **3** (2020). https://doi.org/10.17632/cp3473x7xv.3. https://data.mendeley.com/datasets/cp3473x7xv/3
40. Zhou, H., et al.: Informer: Beyond efficient transformer for long sequence time-series forecasting (2021). http://arxiv.org/abs/2012.07436
41. Vaswani, A., et al.: Attention is all you need, vol. 30 (2017)